Supporting Information:

The impact of solvation on the structure and electric field strength in Li^+GlyGly complexes

Katharina A. E. Meyer and Etienne Garand*

University of Wisconsin-Madison, Department of Chemistry, 1101 University Ave, Madison, WI 53706.
E-mail: egarand@wisc.edu

Contents

List of Tables

List of Figures

1 Computational Methods

A detailed list of keywords used in the harmonic vibrational frequency calculations as well as wavenumber scaling factors can be found in Table S1. Relative DLPNO-CCSD(T)/aVQZ* single-point energies based on the lowest-energy structures of the $Li^+GlyGly\text{-}nH_2O$ complexes with $n = 0-2$ calculated using various methods are listed in Table S2 and a basis set progression of zero-point corrected DLPNO-CCSD(T)/aVXZ//MP2/aVTZ* energies and Gibbs free energies is shown in Figure S1. To validate that the impact on the band position predictions upon the inclusion of the weakly bound D_2 messenger tag is small, we list the band position deviations of scaled harmonic B3LYP-D3(BJ)/def2TZVP calculations of $Li^+GlyGly\text{-}nH_2O$ and $Li^+GlyGly\text{-}nH_2O\text{-}1D_2$ ($n = 0, 1$) with respect to experiment in Table S3. The differences in the average absolute deviations including all observed vibrational modes with and without the inclusion of the tag are with just 0.1 cm^{-1} very small (14.0 cm^{-1} with D_2 and 14.1 cm^{-1} without).

Table S1: Keywords used in harmonic vibrational frequency (DFT and MP2) and single-point calculations (DLPNO-CCSD(T)) performed with GAUSSIAN 16 (version C.01)[1] and ORCA (version 4.2.1).[2–4] Note that for M06-2X, additional calculations using the finer *superfine* integration grid have been carried out to test the integration grid sensitivity of the method. If not otherwise noted, only results using the coarser *ultrafine* integration grid are displayed and all M06-2X calculations in the main text have been carried out with the *ultrafine* integration grid. In addition, the wavenumber scaling factor *WNSF* is listed. *WNSF* is determined with respect to the experimental band position of the OH stretching vibration of the [Oa,Oc] conformer of $Na^+GlyGly$ (3556 cm^{-1}), see ref. [5] for further details.

Method	**Program**	**Keywords**	***WNSF***
B3LYP-D3(BJ)	GAUSSIAN	`B3LYP EmpiricalDispersion=GD3BJ def2TZVP Opt=Tight Integral(Grid=UltraFineGrid) DenFit Freq`	0.964
B3LYP	GAUSSIAN	`B3LYP def2TZVP Opt=Tight Integral(Grid=UltraFineGrid) DenFit Freq`	0.964
ωB97XD	GAUSSIAN	`wB97XD def2TZVP Opt=Tight Integral(Grid=UltraFineGrid) DenFit Freq`	0.939
M06-2X	GAUSSIAN	`M062X def2TZVP Opt=Tight Integral(Grid=UltraFineGrid) DenFit Freq`	0.945
M06-2X	GAUSSIAN	`M062X def2TZVP Opt=Tight Integral(Grid=SuperFineGrid) DenFit Freq`	0.945
PM3	GAUSSIAN	`PM3 Opt=Tight DenFit Freq`	0.933

RI-B2PLYP-D3(BJ)	ORCA	`RI-B2PLYP D3BJ aug-cc-pVTZ AutoAux D3BJ GRID5 NOFINALGRID VERYTIGHTSCF TIGHTOPT NUMFREQ printbasis`
		`%basis`
		`newgto Li "cc-pwCVTZ" end`
		`end`
			0.958

RI-MP2	ORCA	`RI-MP2 aug-cc-pVTZ AutoAux VERYTIGHTSCF TIGHTOPT NUMFREQ printbasis`
		`%basis`
		`newgto Li "cc-pwCVTZ" end`
		`end`
			0.958

DLPNO-CCSD(T)	ORCA	`DLPNO-CCSD(T) aug-cc-pVXZ AutoAux TIGHTSCF TightPNO printbasis`
		`%basis`
		`newgto Li "cc-pwCVXZ" end`
		`end`	

Table S2: Relative energy difference of DLPNO-CCSD(T)/aVQZ* single-point energies of the lowest-energy conformers of $Li^+GlyGly$-nH_2O ($n = 0-2$) on structures optimised with DFT and MP2 (cf. Figure 2 of main text and Figure S2 for structures).

	$Li^+GlyGly$		$Li^+GlyGly$-$1H_2O$			$Li^+GlyGly$-$2H_2O$		
Conformer	**[Oa,Oc]**	**[N,Oa,Oc]**	**[Oa,Oc,W]**	**[W_N,Oa,Oc]**	**[N,Oa,W_{Oc}]**	**[W,N,Oa,W_{Oc}]**	**[Oa,Oc,W,W]**	**[W_N,Oa,Oc,W]**
B3LYP-D3(BJ)/def2TZVP	0.2	0.3	0.4	0.5	0.5	0.7	0.8	0.7
B3LYP/def2TZVP	0.6	0.6	0.7	1.3	0.8	1.6	1.4	1.3
ωB97XD/def2TZVP	1.4	1.0	1.5	1.4	1.4	1.9	2.3	1.9
M06-2X/def2TZVP	0.5	0.6	0.7	1.3	1.0	1.5	1.3	1.3
M06-2X/def2TZVP *superfine*	0.5	0.6	0.7	1.3	0.9	1.4	1.3	1.4
B2PLYP-D3(BJ)/aVTZ*	0.0	0.0	0.0	0.0	0.0	0.0	0.0	0.0
MP2/aVTZ*	0.2	0.2	0.2	0.2	0.3	0.2	0.3	0.3
PM3	46.3	57.1	52.2	45.5	44.5	43.9	55.5	43.5

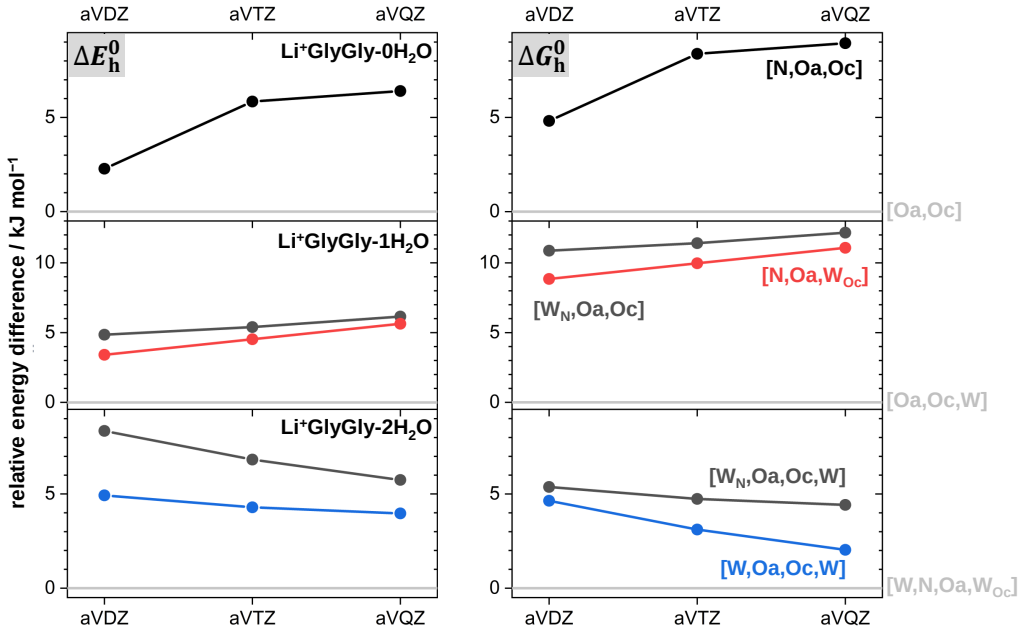

Fig. S1: Relative harmonic, zero-point corrected energy differences ΔE_h^0 (left) and relative Gibbs free energy differences ΔG_h^0 (right) of different conformers of $Li^+GlyGly$-nH_2O complexes with $n = 0-2$ at the DLPNO-CCSD(T)/aVXZ*//MP2/aVTZ* level as a function of the basis set size with X=D, T, and Q. Note that the energies have not been corrected for the basis set superposition error (BSSE), whereas all other energies displayed throughout this work have been BSSE corrected. The conformers are displayed in Figure S2.

Table S3: Deviations of scaled (×0.964) harmonic vibrational frequency calculations of $Li^+GlyGly$-nH_2O and $Li^+GlyGly$-nH_2O-$1D_2$ with $n = 0, 1$ at the B3LYP-D3(BJ)/def2TZVP level with respect to experiment for different types of vibrations (in cm^{-1}). Δ_{OH} marks the deviation for the OH stretch, $\Delta_{NH_2^{a,s}}$ marks deviations for the antisymmetric and symmetric NH_2 stretches, Δ_{NH^b} represents the deviation for the hydrogen bonded NH stretch, and $\Delta_{H_2O^{s,a,b,f}}$ represents the deviations for the symmetric, antisymmetric, hydrogen bonded and free H_2O stretching vibrations. The average absolute deviations over all modes with and without the inclusion of the D_2 tag are with 14.0 cm^{-1} and 14.1 cm^{-1} very similar.

Complex	**Conformer**	Δ_{OH}	$\Delta_{NH_2^a}$	$\Delta_{NH_2^s}$	Δ_{NH^b}	$\Delta_{H_2O^s}$	$\Delta_{H_2O^a}$	$\Delta_{H_2O^b}$	$\Delta_{H_2O^f}$
$Li^+GlyGly$	[Oa,Oc]	1.5	22.0	11.7	21.7				
$Li^+GlyGly$-$1H_2O$	[Oa,Oc,W]	1.3	24.2	14.2	21.4	−7.8	−6.4		
	[N,Oa,W_{Oc}]	4.4						−45.9	−0.7
$Li^+GlyGly$-$1D_2$	[Oa,Oc]	2.7	22.2	11.8	24.7				
$Li^+GlyGly$-$1H_2O$-$1D_2$	[Oa,Oc,W]	0.0	22.4	12.4	21.4	−7.1	−3.5		
	[N,Oa,W_{Oc}]	2.6						−49.2	−2.3

2 Spectral analysis of the $Li^+GlyGly\text{-}nH_2O$ spectra

An overview of the assignments of the experimental bands in the $Li^+GlyGly\text{-}nH_2O\text{-}1D_2$ ($n = 0, 1$) and $Li^+GlyGly\text{-}2H_2O$ spectra can be found in Table S4. Harmonic BSSE corrected relative Gibbs free energy differences ΔG_h^0 and BSSE and zero-point corrected relative energy differences ΔE_h^0 of the lowest-energy conformers of $Li^+GlyGly\text{-}1H_2O$ and $Li^+GlyGly\text{-}2H_2O$ calculated using various methods can be found in Tables S5 and S6. Additional higher-energy conformers for the $Li^+GlyGly\text{-}nH_2O$ clusters with $n = 1, 2$ are shown in Figure S2 alongside relative DLPNO-CCSD(T)/aVQZ*//MP2/aVTZ* energy differences.

2.1 Overview over the experimental results

Table S4: Experimental band positions (in cm^{-1}) and conformer assignments.

Complex	Conformer	νNH^b	νNH_2^s	νNH_2^a	νNH^f	νOH	νH_2O^s	νH_2O^a	νH_2O^b	νH_2O^f
$Li^+GlyGly$	[Oa,Oc]	3294	3396	3456		3542				
$Li^+GlyGly\text{-}1H_2O$	[Oa,Oc,W]	3316	3395	3455		3552	3657	3735		
	[N,Oa,W_{Oc}]					3573			3490	3723
$Li^+GlyGly\text{-}2H_2O$	[W,N,Oa,W_{Oc}]				3481	3575	3659	3744	3505	3722
	[Oa,Oc,W,W]	3333				3557	3659	3744		

2.2 Conformer assignments

Table S5: BSSE corrected relative Gibbs free energy differences ΔG_h^0 of the lowest-energy conformers of $Li^+GlyGly\text{-}1H_2O$ and $Li^+GlyGly\text{-}2H_2O$, calculated at the B3LYP-D3(BJ)/def2TZVP, B3LYP/def2TZVP, ωB97XD/def2TZVP, M06-2X/def2TZVP, B2PLYP-D3(BJ)/aVTZ*, and MP2/aVTZ* levels. Additional single-point calculations were performed at the DLPNO-CCSD(T)/aVQZ* level on the MP2/aVTZ geometries, which are listed using MP2/aVTZ* zero-point and thermal corrections.

		ΔG_h^0						
		B3LYP-D3	**B3LYP**	**ωB97XD**	**M06-2X**	**B2PLYP-D3**	**MP2**	**DLPNO-CCSD(T)**
$Li^+GlyGly\text{-}1H_2O$	[Oa,Oc,W]	0.0	0.0	0.0	0.0	0.0	0.0	0.0
	[W_N,Oa,Oc]	17.2	23.4	17.3	14.2	12.3	12.9	13.3
	[N,Oa,W_{Oc}]	18.1	23.0	16.3	13.4	13.0	10.0	11.8
$Li^+GlyGly\text{-}2H_2O$	[Oa,Oc,W,W]	0.0	0.0	0.0	0.0	0.1	2.4	1.1
	[W_N,Oa,Oc,W]	6.1	11.5	5.3	6.0	3.0	5.6	4.8
	[W,N,Oa,W_{Oc}]	3.3	7.7	1.3	2.2	0.0	0.0	0.0

Table S6: Zero-point and BSSE corrected relative energy differences ΔE_h^0 of the lowest-energy conformers of $Li^+GlyGly\text{-}1H_2O$ and $Li^+GlyGly\text{-}2H_2O$, calculated at the B3LYP-D3(BJ)/def2TZVP, B3LYP/def2TZVP, ωB97XD/def2TZVP, M06-2X/def2TZVP, B2PLYP-D3(BJ)/aVTZ*, and MP2/aVTZ* levels. Additional single-point calculations were performed at the DLPNO-CCSD(T)/aVQZ* level on the MP2/aVTZ geometries, which are listed using MP2/aVTZ* zero-point and thermal corrections.

		ΔE_h^0						
		B3LYP-D3	**B3LYP**	**ωB97XD**	**M06-2X**	**B2PLYP-D3**	**MP2**	**DLPNO-CCSD(T)**
$Li^+GlyGly\text{-}1H_2O$	[Oa,Oc,W]	0.0	0.0	0.0	0.0	0.0	0.0	0.0
	[W_N,Oa,Oc]	6.9	13.5	5.2	2.1	6.8	6.9	7.3
	[N,Oa,W_{Oc}]	9.9	15.4	5.8	2.2	8.3	4.5	6.4
$Li^+GlyGly\text{-}2H_2O$	[Oa,Oc,W,W]	3.4	0.0	5.9	8.3	3.9	6.2	4.9
	[W_N,Oa,Oc,W]	1.4	4.0	3.4	3.9	2.4	5.1	4.4
	[W,N,Oa,W_{Oc}]	0.0	1.4	0.0	0.0	0.0	0.0	0.0

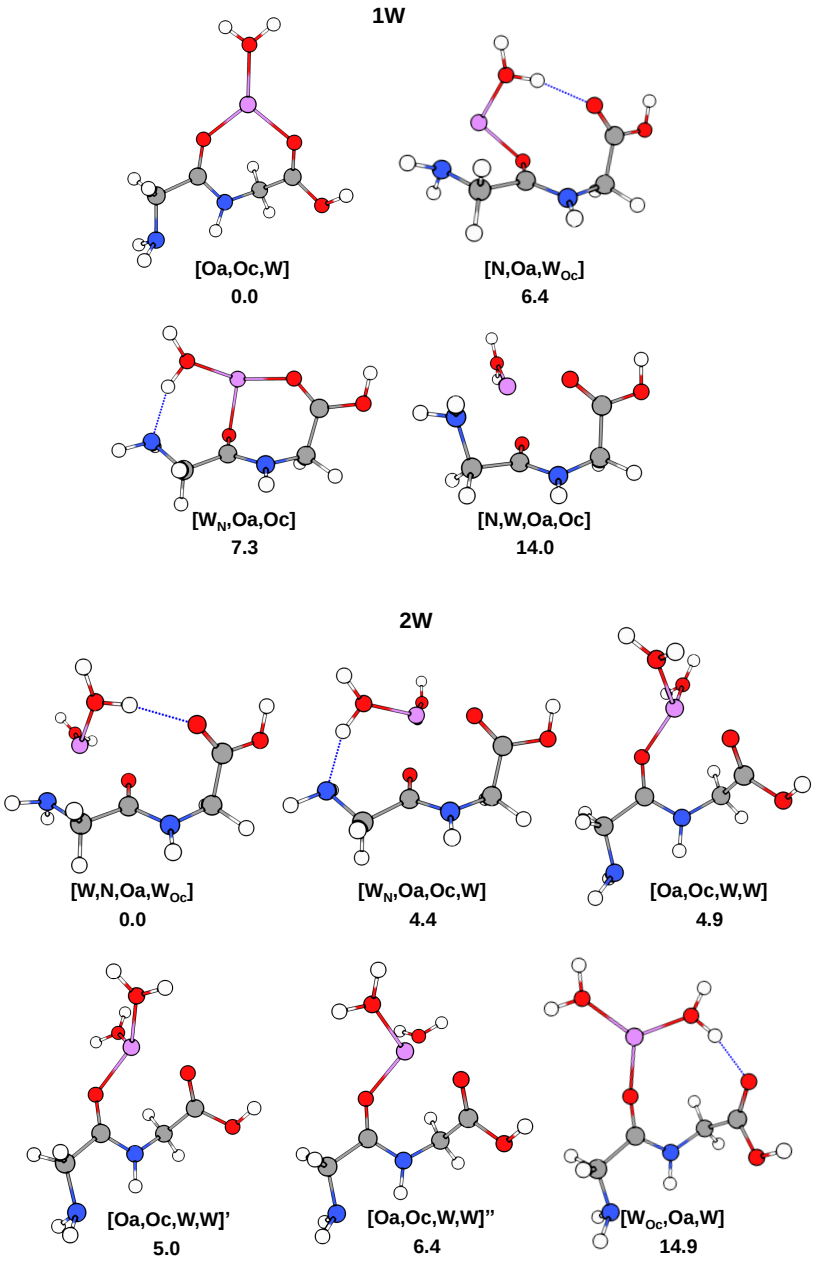

Fig. S2: Structures of the lowest-energy conformers of $Li^+GlyGly\text{-}nH_2O$ complexes with $n = 1$ and 2 alongside relative harmonic and zero-point corrected energy differences ΔE_h^0 at the DLPNO-CCSD(T)/aVQZ*//MP2/aVTZ* level.

3 Agreement between experiment and theory

Table S7 lists the deviations between scaled harmonic vibrational frequency calculations and experiment for various methods including all vibrational modes assigned in the spectra (cf. Table S4). Compared to Table 1 in the main text, this table also includes the deviations for the symmetric and antisymmetric NH_2 stretching vibrations and the results for M06-2X/def2TZVP calculations using the finer *superfine* integration grid. The agreement between experiment and theory seems to improve for B3LYP-D3(BJ) if the dispersion correction is omitted. As seen in Table S2, the relative DLPNO-CCSD(T)/aVQZ* energy difference of the B3LYP structure with respect to B2PLYP-D3(BJ) is higher than that of the B3LYP-D3(BJ) structure, meaning that it is further away from the DLPNO-CCSD(T)/aVQZ* minimum. The improved vibrational description on a seemingly less-accurate structure could either be a geometric effect or a result of a better vibrational description. To investigate this, we have carried out a harmonic vibrational frequency calculation including the D3(BJ) dispersion on a geometry obtained without this correction and *vice versa* (*e.g., B3LYP-D3(BJ)//B3LYP*). The results of these calculations for the lowest-energy $Li^+GlyGly\text{-}1H_2O$ and $Li^+GlyGly\text{-}2H_2O$ conformers can be found in Tables S8 and S9, respectively. The resulting band positions of these cross-calculations resemble the 'pure' calculation (same method for the geometry optimisation and Hessian) that has the same geometry, indicating that the improvement of the vibrational frequencies by omitting the dispersion correction is largely a geometric effect.

Table S7: Total CPU times t_{CPU} (in h), average absolute deviations of scaled harmonic vibrational frequency calculations over all vibrational modes assigned in the $Li^+GlyGly\text{-}nH_2O\text{-}1D_2$ ($n = 0, 1$) and $Li^+GlyGly\text{-}2H_2O$ spectra ($\overline{|\Delta_{oa}|}$), and average deviations obtained for the OH $\overline{\Delta_{OH}}$, antisymmetric and symmetric NH_2 $\overline{\Delta_{NH_2^{a,s}}}$, hydrogen bonded NH $\overline{\Delta_{NH^b}}$, as well as free, antisymmetric, symmetric, and hydrogen bonded H_2O vibrations $\overline{\Delta_{H_2O^{f,a,s,b}}}$ (all in cm^{-1}). The average deviations are displayed alongside their standard deviations in parenthesis. The free NH stretching vibration $\nu(NH)^f$ has only been observed for $Li^+GlyGly\text{-}2H_2O$ ([W,N,Oa,W_{Oc}] conformer) and is therefore displayed without a standard deviation (Δ_{NH^f}). Note that the asterisk (*) at the aVTZ* basis set indicates that for Li^+, the aVTZ basis set has been replaced with the weighted core-valence cc-pwCVTZ basis set.

Method	t_{CPU}	$\overline{\lvert\Delta_{oa}\rvert}$	$\overline{\Delta_{OH}}$	$\overline{\Delta_{NH_2^a}}$	$\overline{\Delta_{NH_2^s}}$	Δ_{NH^f}	$\overline{\Delta_{NH^b}}$	$\overline{\Delta_{H_2O^{f,a,s}}}$	$\overline{\Delta_{H_2O^b}}$
B3LYP-D3(BJ)/def2TZVP	10.5	11.1	3(1)	23(2)	13(2)	3.2	21(0)	−2(4)	−39(10)
B3LYP/def2TZVP	11.3	8.7	2(1)	22(1)	12(1)	−0.5	19(2)	−3(3)	−22(2)
ωB97XD/def2TZVP	15.2	15.3	−1(1)	−13(0)	−26(0)	−36.6	−3(3)	−12(4)	−61(10)
M06-2X/def2TZVP	16.7	15.4	0(2)	−6(2)	−19(2)	−31.7	17(3)	−17(4)	−37(4)
M06-2X/def2TZVP *superfine*	29.3	16.6	−1(1)	−9(1)	−22(1)	−35.7	18(3)	−18(4)	−37(3)
B2PLYP-D3(BJ)/aVTZ*	6671.3	10.7	0(1)	24(0)	9(0)	2.3	29(3)	−4(4)	−29(1)
MP2/aVTZ*	6614.1	11.9	−1(1)	39(1)	14(1)	10.9	23(2)	4(9)	−10(2)
PM3	0.02	95.8	3(5)	−284(0)	−106(1)	−333.0	−194(16)	−64(30)	3(2)

Table S8: Harmonically calculated band positions of the three lowest-energy Li^+GlyGly-$1H_2O$ conformers using optimised geometries and Hessians computed at the B3LYP-D3(BJ)/def2TZVP and B3LYP/def2TZVP levels. The methods are displayed as geometry optimisation//frequency calculation, meaning B3LYP-D3(BJ)//B3LYP refers to a B3LYP frequency calculation on an optimised B3LYP-D3(BJ) geometry.

Conformer	**Method**	$\omega(\mathbf{H_2O})^a$	$\omega(\mathbf{H_2O})^f$	$\omega(\mathbf{H_2O})^s$	$\omega(\mathbf{OH})$	$\omega(\mathbf{NH})^f$	$\omega(\mathbf{H_2O})^b$	$\omega(\mathbf{NH_2})^a$	$\omega(\mathbf{NH_2})^a$	$\omega(\mathbf{NH})^f$
[Oa,Oc,W]	B3LYP-D3//B3LYP-D3	3869		3786	3685			3610	3537	3461
	B3LYP-D3//B3LYP	3870		3786	3685			3610	3537	3461
	B3LYP//B3LYP	3868		3785	3684			3607	3534	3458
	B3LYP//B3LYP-D3	3868		3785	3684			3607	3534	3458
[N,Oa,W_{Oc}]	B3LYP-D3//B3LYP-D3		3861		3711	3613	3573	3557	3489	
	B3LYP-D3//B3LYP		3862		3711	3613	3573	3557	3489	
	B3LYP//B3LYP		3859		3710	3609	3598	3554	3488	
	B3LYP//B3LYP-D3		3859		3709	3610	3598	3554	3488	
[W_N,Oa,Oc]	B3LYP-D3//B3LYP-D3		3867		3692	3613	3164	3564	3490	
	B3LYP-D3//B3LYP		3868		3693	3613	3164	3564	3490	
	B3LYP//B3LYP		3864		3691	3609	3214	3560	3488	
	B3LYP//B3LYP-D3		3864		3691	3609	3214	3560	3488	

Table S9: Harmonically calculated band positions of the three lowest-energy Li^+GlyGly-$2H_2O$ conformers using optimised geometries and Hessians at the B3LYP-D3(BJ)/def2TZVP and B3LYP/def2TZVP level. The methods are displayed as geometry optimisation//frequency calculation, meaning B3LYP-D3(BJ)//B3LYP refers to a B3LYP frequency calculation on an optimised B3LYP-D3(BJ) geometry.

Conformer	**Method**	$\omega(\mathbf{H_2O})^a$	$\omega(\mathbf{H_2O})^f$	$\omega(\mathbf{H_2O})^s$	$\omega(\mathbf{OH})$	$\omega(\mathbf{NH})^f$	$\omega(\mathbf{H_2O})^b$	$\omega(\mathbf{NH_2})^a$	$\omega(\mathbf{NH_2})^a$	$\omega(\mathbf{NH})^f$
[W,N,Oa,W_{Oc}]	B3LYP-D3//B3LYP-D3	3879	3863	3791	3712	3614	3590	3567	3495	
	B3LYP-D3//B3LYP	3879	3864	3791	3712	3614	3590	3567	3495	
	B3LYP//B3LYP	3876	3861	3790	3711	3611	3610	3564	3494	
	B3LYP//B3LYP-D3	3876	3861	3789	3710	3611	3610	3564	3494	
[Oa,Oc,W,W]	B3LYP-D3//B3LYP-D3	3886, 3882		3796, 3790	3694			3609	3535	3479
	B3LYP-D3//B3LYP	3887, 3882		3796, 3790	3694			3609	3535	3479
	B3LYP//B3LYP	3885, 3883		3794, 3791	3693			3606	3533	3476
	B3LYP//B3LYP-D3	3884, 3883		3794, 3791	3692			3606	3533	3476
[W_N,Oa,Oc,W]	B3LYP-D3//B3LYP-D3	3883	3872	3793	3700	3618	3230	3568	3493	
	B3LYP-D3//B3LYP	3883	3873	3793	3700	3617	3230	3568	3493	
	B3LYP//B3LYP	3880	3869	3792	3699	3613	3274	3564	3491	
	B3LYP//B3LYP-D3	3880	3869	3792	3699	3613	3274	3564	3491	

4 Tentative analysis of the Li^+GlyGly-$3H_2O$ spectra

In Figure S3, the lowest-energy conformers of Li^+GlyGly-$3H_2O$ are shown alongside harmonic, zero-point and BSSE corrected relative energy differences ΔE_h^0 and relative Gibbs free energy differences ΔG_h^0, calculated at the DLPNO-CCSD(T)/aVQZ*//B3LYP-D3(BJ)/def2TZVP level. The wavenumber-scaled, harmonic vibrational spectra calculated at the B3LYP/def2TZVP level are shown in Figure S4.

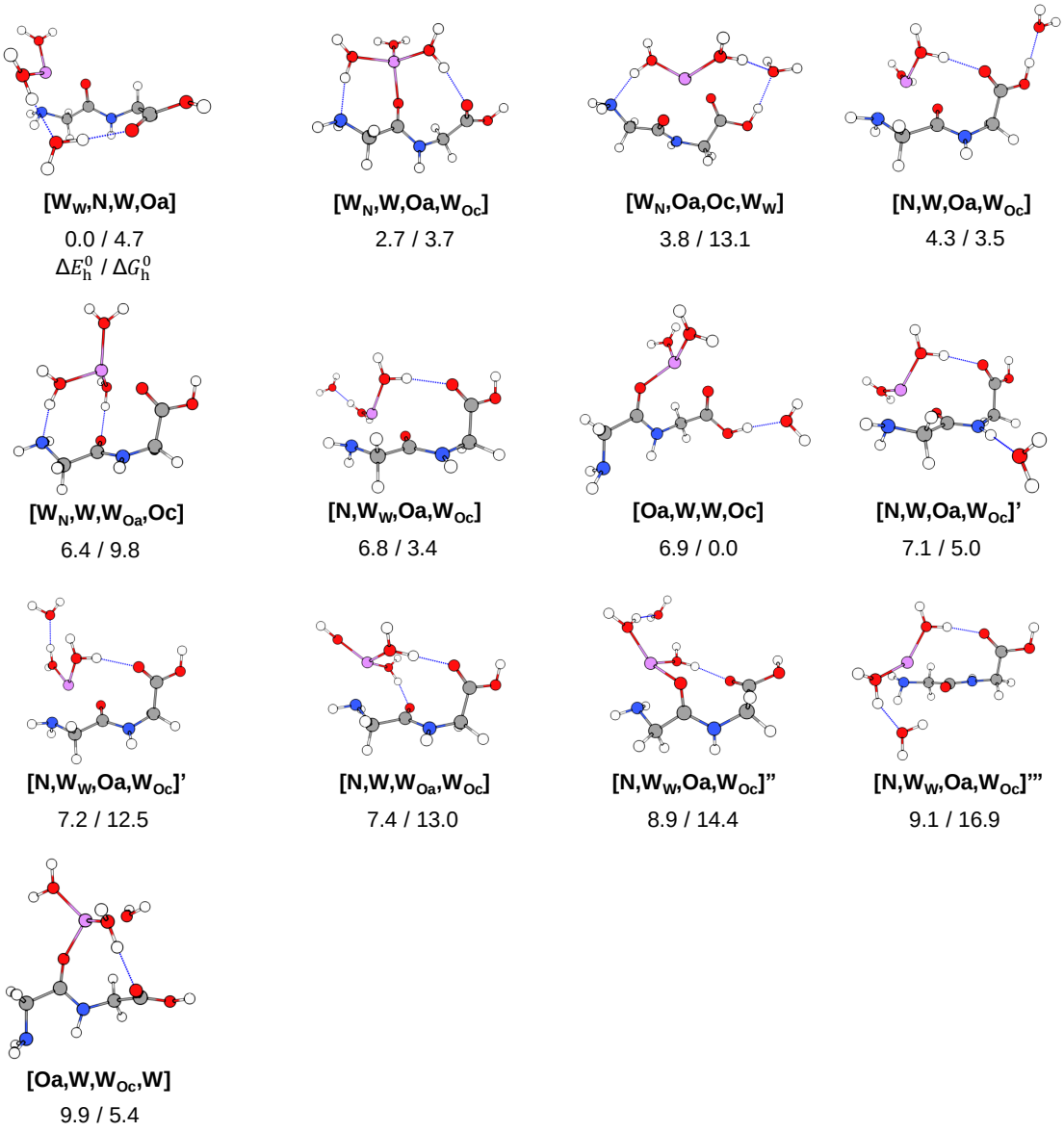

Fig. S3: Lowest-energy conformers of Li^+GlyGly-$3H_2O$. Oa and Oc in the conformer labels indicate metal ion coordination to the amide and carboxylic C=O groups, N metal ion coordination to the lone pair of the NH_2 group, W indicates water coordination to Li^+, and subscripts illustrate the location of hydrogen bonds originating from the respective metal ion binding sites. Harmonic zero-point and BSSE corrected relative energy differences ΔE_h^0 and relative Gibbs free energy differences ΔG_h^0 are listed below the conformers, calculated at the DLPNO-CCSD(T)/aVQZ*//B3LYP-D3(BJ)/def2TZVP level.

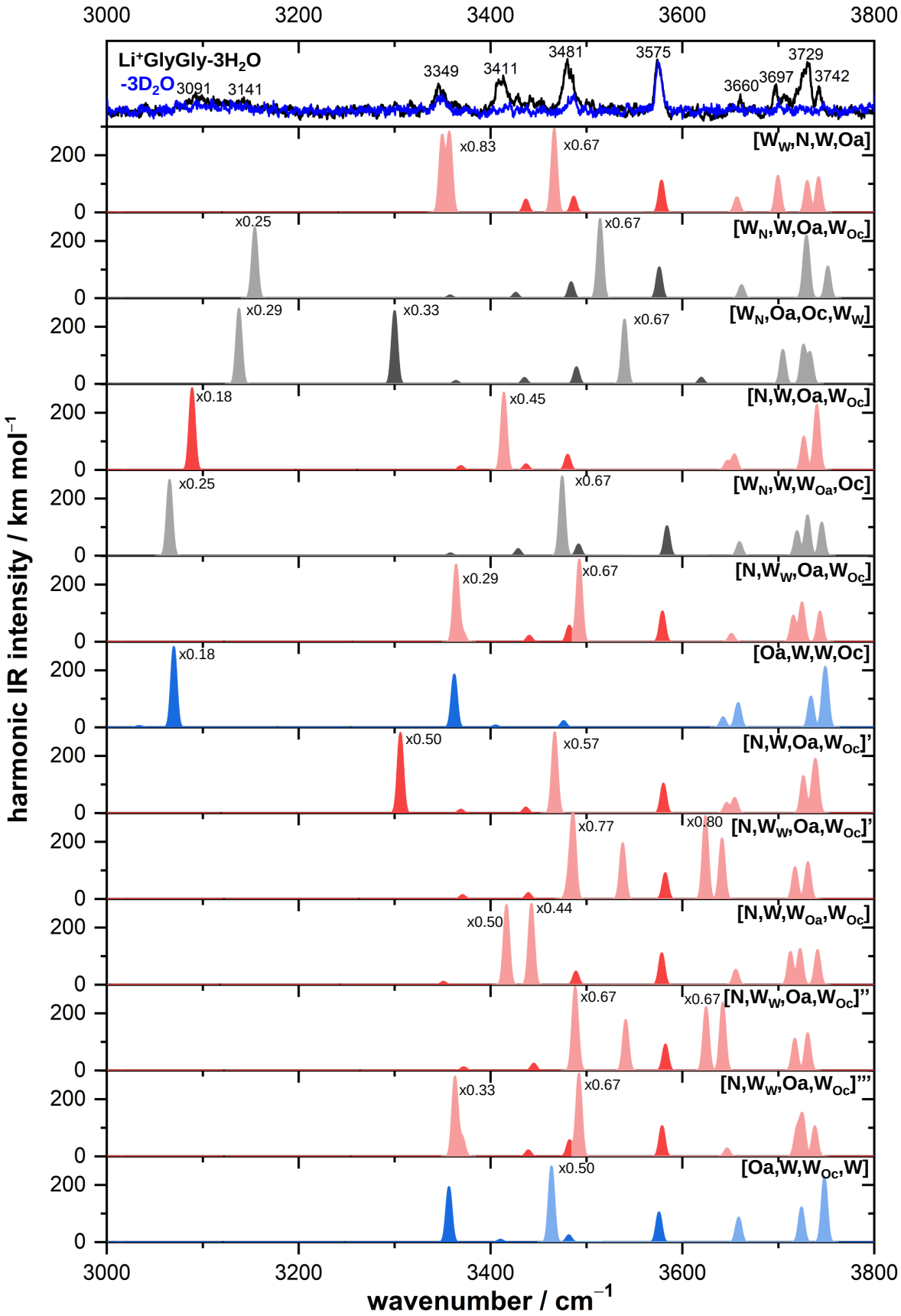

Fig. S4: Infrared action spectra of $Li^+GlyGly$-$3H/D_2O$ alongside harmonically calculated, scaled (×0.964) and Gaussian-broadened ($\sigma = 4\,cm^{-1}$) spectra of the lowest-energy conformers at the B3LYP/def2TZVP level. Predicted bands corresponding to water vibrations are shown in a lighter and peptide vibrations in a darker shade (grey/blue/red), respectively. Note that the spectra were recorded *via* water-loss. BSSE and zero-point corrected relative energy differences and relative Gibbs free energy differences of the different conformers calculated at the DLPNO-CCSD(T)/aVQZ*//B3LYP-D3(BJ)/def2TZVP level can be found in Figure S3 ($\Delta E_h^0/\Delta G_h^0$, in kJ mol^{-1}).

References

[1] M. J. Frisch, G. W. Trucks, H. B. Schlegel, G. E. Scuseria, M. A. Robb, J. R. Cheeseman, G. Scalmani, V. Barone, G. A. Petersson, H. Nakatsuji, X. Li, M. Caricato, A. V. Marenich, J. Bloino, B. G. Janesko, R. Gomperts, B. Mennucci, H. P. Hratchian, J. V. Ortiz, A. F. Izmaylov, J. L. Sonnenberg, D. Williams-Young, F. Ding, F. Lipparini, F. Egidi, J. Goings, B. Peng, A. Petrone, T. Henderson, D. Ranasinghe, V. G. Zakrzewski, J. Gao, N. Rega, G. Zheng, W. Liang, M. Hada, M. Ehara, K. Toyota, R. Fukuda, J. Hasegawa, M. Ishida, T. Nakajima, Y. Honda, O. Kitao, H. Nakai, T. Vreven, K. Throssell, J. A. Montgomery, Jr., J. E. Peralta, F. Ogliaro, M. J. Bearpark, J. J. Heyd, E. N. Brothers, K. N. Kudin, V. N. Staroverov, T. A. Keith, R. Kobayashi, J. Normand, K. Raghavachari, A. P. Rendell, J. C. Burant, S. S. Iyengar, J. Tomasi, M. Cossi, J. M. Millam, M. Klene, C. Adamo, R. Cammi, J. W. Ochterski, R. L. Martin, K. Morokuma, O. Farkas, J. B. Foresman, D. J. Fox, Gaussian 16 Revision C.01, Gaussian Inc. Wallingford CT, **2019**.
[2] F. Neese, *Wiley Interdiscip. Rev. Comput. Mol. Sci.* **2012**, *2*, 73–78.
[3] F. Neese, *Wiley Interdiscip. Rev. Comput. Mol. Sci.* **2018**, *8*, e1327.
[4] F. Neese, F. Wennmohs, U. Becker, C. Riplinger, *J. Chem. Phys.* **2020**, *152*, 224108.
[5] K. A. E. Meyer, K. A. Nickson, E. Garand, *J. Chem. Phys.* **2022**, *157*, 174301.